

A NOVEL DUAL MODE SUBSTRATE INTEGRATED WAVEGUIDE FILTER WITH MIXED SOURCE-LOAD COUPLING (MSLC)

Ziqiang Xu^{1, *}, Yu Shi², Congyu Xu¹, and Peng Wang¹

¹Research Institute of Electronic Science and Technology, University of Electronic Science and Technology of China, Chengdu 611731, China

²State Key Laboratory of Electronic Thin Films and Integrated Devices, University of Electronic Science and Technology of China, Chengdu 611731, China

Abstract—A novel single-cavity dual mode substrate integrated waveguide (SIW) filter with mixed source-load coupling (MSLC) is presented. By using an interdigital slot-line (ISL) to introduce mixed coupling between source and load, the proposed filter with only one cavity could have three transmission zeros which can be controlled flexibly. Under the circumstances, the filter exhibits better frequency selectivity in comparison with conventional dual mode SIW filters. An experimental filter with a center frequency of 10 GHz and a 3 dB fractional bandwidth of 6.0% is designed, fabricated, and measured to validate the proposed structure. Measured results are provided to show good performance and in agreement with the simulated ones.

1. INTRODUCTION

Rapid development of wireless and mobile communication systems needs more and more bandpass filters with stringent frequency selectivity, low profile, and wide stopband [1, 2]. Microwave dual-mode filters with high performance and compact size have been widely used and been implemented by metal waveguide and microstrip in various communication systems [3]. The metal waveguide dual mode filters have excellent performance owing to their high Q factor and power-handling capability [4]. However, they cannot be easily integrated with microwave planar circuits. Also, a high precision mechanical adjustment or a subtle tuning mechanism is needed to obtain satisfying

Received 15 December 2012, Accepted 21 January 2013, Scheduled 23 January 2013

* Corresponding author: Ziqiang Xu (nanterxu@uestc.edu.cn).

filters [5–7]. Although the microstrip dual-mode filters are easily designed and integrated into the high density layouts, they have lower resonator Q factor and lower power-handing capability [8, 9]. Recently the substrate integrated waveguide (SIW), which is synthesized in a planar substrate with arrays of metallic via, has provided a useful technology to design low-profile, low-cost, and easy integration waveguide filters [10, 11]. SIW filters can be fabricated by using the printed circuit board (PCB) or LTCC processes [12, 13]. Various SIW filters with high performances are designed and implemented, such as evanescent-mode [14], half mode [15], coplanar waveguide incorporating [16], extended doublet [17], mixed cross coupling [18] and folding [19], etc.. Particularly, the application of SIW technology makes the implement of dual mode cavity filters with compact size and easy integration possible [20].

On the other hand, filters with multiple transmission zeros are required to meet the increasing demands of modern communication systems in regards to high frequency selectivity. Ordinarily, no more than one transmission zero can be obtained in a conventional single-cavity dual mode filter. A dual-mode SIW filter with one transmission zero has been implemented by using an orthogonal input and output feed-line and two tuning metal vias for disturbing two degenerate modes [21]. In order to generate more transmission zeros, many approaches have been proposed to design dual mode SIW filters. In [22], a dual-mode SIW filter has been realised by slot lines perturbation, and there are two finite frequency transmission zeros allocated at each side of its passband. In [23], a single-cavity dual-mode filter which used a coplanar waveguide as a non-resonating node (NRN) is proposed, and two transmission zeros can be obtained due to the indirect cross-coupling. Besides, a SIW filter with cascading two adjacent dual-mode resonators is designed to generate up to two transmission zeros in [24]. Similarly, by constructing with two circular cavities, a dual mode filter with two transmission zeros at upper side of the passband is presented in [25].

In this paper, to achieve better frequency selectivity without enlarging sizes of the filter, a novel single-cavity dual mode SIW filter with an interdigital slot-line (ISL) is investigated theoretically and experimentally. By introducing mixed coupling between source and load, the filter not only has three transmission zeros to improve frequency selectivity, but also has a small size by profit from its single-cavity structure. In order to validate the structure of the proposed model, an experimental filter configuration at the central frequency of 10 GHz are fabricated and measured. Design details are described, and both computed and experimental results are presented and discussed.

2. FILTER ANALYSIS AND DESIGN

2.1. Topology Diagram

Figures 1(a) and (b) show the comparison between the conventional and proposed modified topology, where the empty disks symbolize the source/load, and the dark disks represent two resonant modes (TE_{102}/TE_{201}) behaving as resonators 1 and 2, respectively. Conventional topology of a transversal doublet without source-load coupling can obtain only one transmission zero in either side of the passband. By adding source and load coupling into the doublet, a modified doublet (MD) is proposed to achieve two transmission zeros [26]. Under the circumstances, with introducing mixed coupling between the source and the load, another transmission zeros can be obtained, which is shown in Figure 1(c). The coexistence of electric and magnetic coupling can be adopted to build dual-coupling paths between source and load to introduce additional transmission zero, which are usually controllable by adjusting the mixed coupling coefficients. In other words, the source and the load are directly

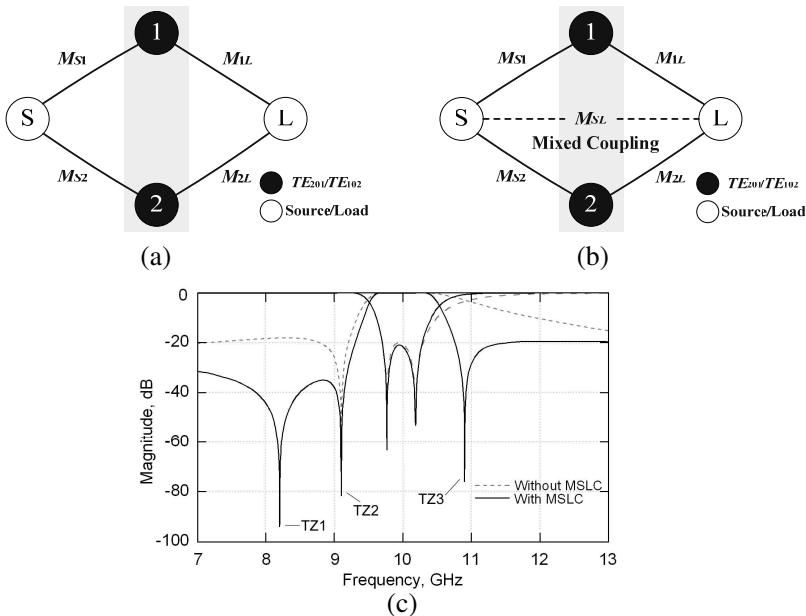


Figure 1. Coupling schemes and frequency response of single-cavity dual-mode filter with and without mixed source-load coupling (MSLC). (a) Conventional topology, (b) modified topology and (c) frequency response.

coupled which can add an additional transmission path based on conventional transversal doublet, and then mixed coupling between them can also bring another signal path to generate up to three transmission zeros [27]. The coupling matrix M of the proposed topology can be written as

$$M = \begin{bmatrix} 0 & M_{S1} & M_{S2} & M_{SL}(\omega) \\ M_{S1} & M_{11} & 0 & M_{1L} \\ M_{S2} & 0 & M_{22} & M_{2L} \\ M_{SL}(\omega) & M_{1L} & M_{2L} & 0 \end{bmatrix} \quad (1)$$

where M_{S1} , M_{S2} , M_{1L} and M_{2L} express the coupling between source/load and each resonator mode, respectively. M_{11} and M_{22} of diagonal elements in coupling matrix account for differences in the resonant frequencies of the resonators. $M_{SL}(\omega)$ represents the mixed coupling between source and load, which is composed of electric and magnetic coupling. $M_{SL}(\omega)$ can be obtained by using the conventional solution method of a mixed coupling coefficient, as described in [27]

$$M_{SL}(\omega) = [\omega L_m - 1/(\omega C_m)]/\omega_0 L \quad (2)$$

where each resonator in the equivalent circuit of the two mixed coupled resonators is characterized by a parallel capacitance C together with an inductance L and its resonant frequency equals to $\omega_0 = (LC)^{-1/2}$. C_m and L_m denote the coupling capacitance and inductance and they will produce mixed electric and magnetic coupling, respectively. Besides, the coupling coefficient at center frequency ω_0 is written as

$$k(\omega_0) = L_m (1 - \omega_m^2/\omega_0^2) / L \quad (3)$$

where $\omega_m = (L_m C_m)^{-1/2}$. In addition, it also has

$$M_{SL}(\omega) = k(\omega_0)\omega_0 (\omega^2 - \omega_m^2) / [\omega (\omega_0^2 - \omega_m^2)] \quad (4)$$

Here, it can be noticed that mixed coupling coefficient is relative to frequency. It can be either positive or negative which can be considered separately for predigestion. When the mixed coupling coefficient is positive, namely, the infinite C_m inclines ω_m to 0. Then the coupling coefficient can be described as:

$$M_{SL}(\omega) = \omega L_m/\omega_0 L = \omega k(\omega_0)/\omega_0 \quad (5)$$

Meanwhile, when the coupling coefficient is negative, L_m inclines to 0, and ω_m inclines to infinite as a result. Then the coupling coefficient can be given as:

$$M_{SL}(\omega) = \omega_0 C/\omega C_m = \omega_0 k(\omega_0)/\omega \quad (6)$$

To achieve above mentioned topology, a dual mode SIW filter is proposed in a PCB substrate as shown in Figure 2. The single cavity

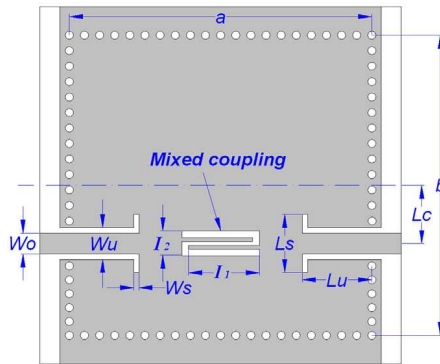


Figure 2. The configurations of proposed dual mode filter.

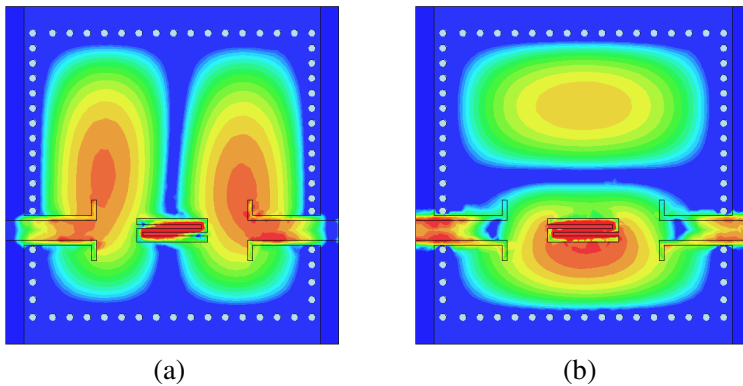


Figure 3. The E -field distributions of (a) vertical mode and (b) horizontal mode.

resonator operates with TE_{102}/TE_{201} modes, and the ISL structure on the top metal layer is implemented to introduce mixed coupling between source and load [18]. Feeding structures with input/output current probes are offset from the center line of the SIW to excite the two resonant modes. Figure 3 shows the E -field distributions of vertical and horizontal modes in the single cavity dual-mode resonator.

2.2. Location of Transmission Zeros

To get more insight of location of transmission zero in this mixed coupling MD, an explicit expression relating the coupling elements and the transmission zero is given by

$$\Omega = a \pm (b^2 + c^2)^{1/2} \tag{7a}$$

where

$$a = (M_{S1}^2 + M_{S2}^2) / 2M_{SL} - (M_{11} + M_{22}) / 2 \quad (7b)$$

$$b = (M_{S2}^2 - M_{S1}^2) / 2M_{SL} - (M_{11} - M_{22}) / 2 \quad (7c)$$

$$c = M_{S1}M_{S2} / M_{SL} \quad (7d)$$

where $\Omega = (\omega/\omega_0 - \omega_0/\omega) / FBW$ is normalized angular frequency while FBW is the fractional bandwidth. Because M_{SL} is mixed coupling related with frequency based on (4), it has

$$M_{SL} = M_{SL}(\omega_0)\omega_0 (\omega^2 - \omega_m^2) / [\omega (\omega_0^2 - \omega_m^2)] \quad (7e)$$

Here, it can be seen that conventional transversal doublet without source-load coupling can obtain only one transmission zero below or above its passband. By introducing MSLC with frequency-variant coupling to MD, as shown in Figure 1(a), two extra controllable transmission zeros will be generated in the stopband. Meanwhile, the levels of electric and magnetic coupling of MSLC which can tune the locations of TZs are mainly controlled by the length (I_1) and the width (I_2) of ISL. Moreover, the resonant frequency of the ISL is far from the central frequency so the ISL almost does not affect the passband of the filter. Figure 4(a) illustrates the S_{21} -parameter of proposed dual mode SIW filter for different values of I_1 . Transmission zeros TZ2 and TZ3 located at each side of its passband are mainly dominated by primary MD structure. Hence locations of TZ2 and TZ3 change slightly when varying the values of I_1 . However, as an additional transmission zero caused by mixed coupling, TZ1 is much more sensitive to the values of I_1 , namely, TZ1 characterized by $\omega_m = (L_m C_m)^{-1/2}$ will be produced by the mixed coupling between the source and load, and it has an obvious relationship with ω_0 as follows

$$\omega_0/\omega_m = (k_m/k_c)^{1/2} = (L_m C_m / LC)^{1/2} \quad (8)$$

where $k_m L_m L$ is the magnetic coupling part while $k_c C C_m$ is the electric coupling one. With increasing the values of I_1 , i.e., adding coupling capacitance C_m , the electric coupling part ($C C_m$) of the mixed coupling will become weaker. Meanwhile, the increase of C_m will result in the decrease of ω_m , as shown in Figure 4(a), the additional transmission zero at the lower stopband moves to lower frequencies.

On the other hand, the offset L_c between the center line and feeding structure of the single-cavity SIW filter also has obvious influence on the locations of the transmission zeros, especially to TZ3. Figure 4(b) shows the S_{21} -parameter of the proposed filter for different values of L_c . With increasing the values of L_c , TZ3 at the upper stopband shifts towards the higher frequencies, whereas positions of

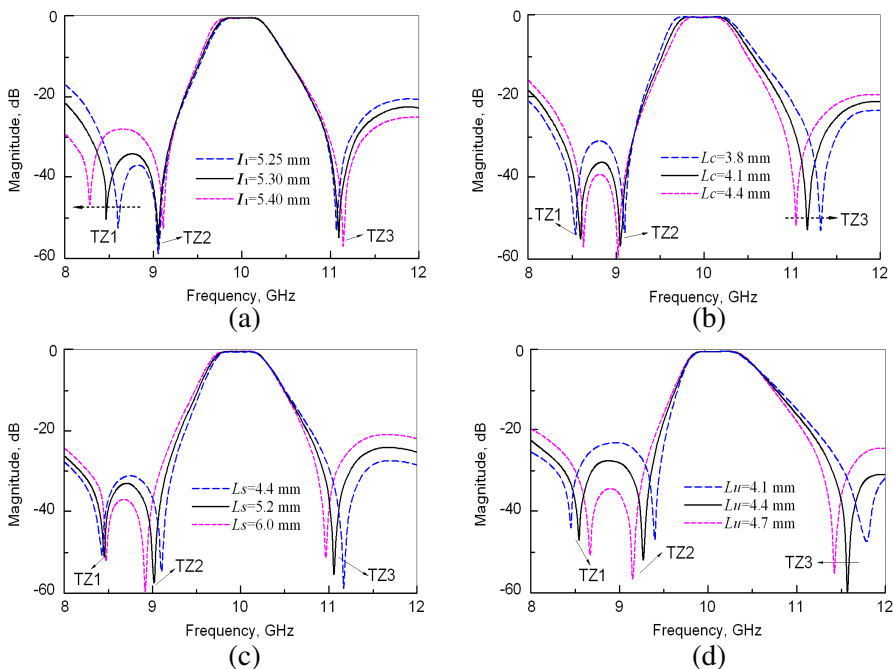


Figure 4. S_{21} -parameters as a function of frequency for different values of (a) I_1 , (b) L_c , (c) L_s and (d) L_u , respectively.

TZ1 and TZ2 at the lower stopband move slightly. Besides, the length and width of input/output current probes in feeding structure will have evident effect on the locations of transmission zeros and bandwidth of the filter. Figures 4(c) and (d) show the S_{21} -parameter of the proposed filter for different values of lengths L_s and L_u of input/output current probes, respectively. It can be seen that the values of L_s and L_u influence three transmission zeros obviously. With the values of L_s and L_u increase, TZ1 and TZ3 show a general tendency to move toward the center of passband, while on the contrary TZ2 shifts away from the center of passband. Furthermore, it should be noted that width of input/output current probes in feeding structure can also affect in-band return loss of the filter. Figures 5(a) and (b) show the S_{11} -parameter of the proposed filter for different values of widths W_u and W_s of input/output current probes, respectively. To achieve demanded frequency responses during design process of the proposed dual-mode SIW filter, mixed coupling structure and feeding probes ought to be controlled and tuned together.

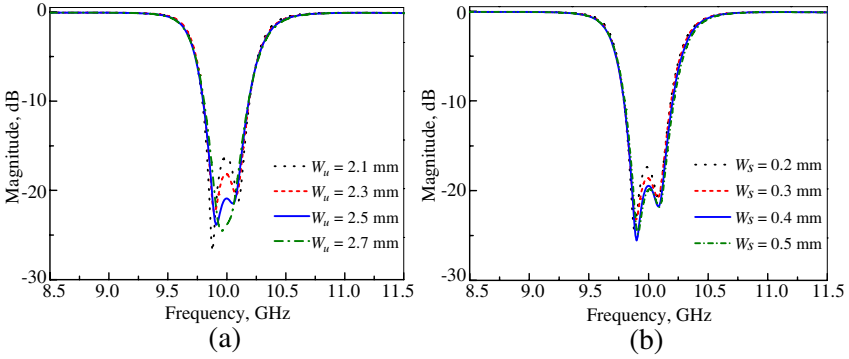


Figure 5. S_{11} -parameters as a function of frequency for different values of (a) W_u and (b) W_s , respectively.

2.3. Single-cavity Dual-mode Filter Design

To demonstrate the application of above-mentioned structure, a single-cavity dual-mode SIW filter is designed to have a central frequency of 10 GHz, a 3 dB fractional bandwidth of 6%, and three transmission zeros which are located at 8.2, 9.2 and 10.8 GHz, respectively. The substrate used for the proposed filter is Rogers 5880, and its relative permittivity is 2.2 with a thickness of 0.508 mm.

The initial sizes of single-cavity dual mode SIW resonator can be calculated by using the following equation

$$f_{res} = \frac{c}{2\pi\sqrt{\epsilon_r}} \sqrt{\left(\frac{m}{L_{eff}}\right)^2 + \left(\frac{n}{W_{eff}}\right)^2} = \frac{c}{2\pi\sqrt{\epsilon_r}} \sqrt{\left(\frac{p}{L_{eff}}\right)^2 + \left(\frac{q}{W_{eff}}\right)^2} \quad (9)$$

where m , n , p and q are indices of the mode, the only additional constrain of the dual-mode operation is that $m \neq p$ and $n \neq q$. For a square SIW cavity, its TE_{201} and TE_{102} modes resonate at the same frequency. c is the velocity of light in the vacuum, ϵ_r is the relative dielectric constant, L_{eff} and W_{eff} are the effective length and width of the resonant cavity given by

$$L_{eff} = l - \frac{d^2}{0.95p}, \quad W_{eff} = w - \frac{d^2}{0.95p}, \quad (10)$$

where l and w are the length and width of resonant cavity, respectively; d and p are the diameter of metallic via and the space between adjacent vias, respectively [6]. Base on the primary parameters from calculations, the complete filter parameters are fine tuned by slight alterations of each cavity resonator related the actual LTCC process and each coupling in turn until the filter response is optimized to achieve the desired response by using commercial full wave electromagnetic simulation software HFSS.

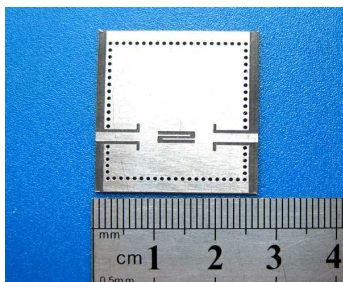


Figure 6. Photograph of fabricated filter.

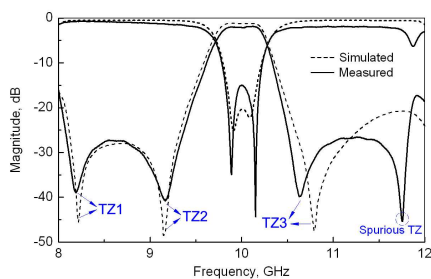


Figure 7. Measured and simulated frequency responses of the proposed filter.

3. EXPERIMENTAL RESULTS

The proposed single-cavity dual mode SIW filter has been fabricated on a PCB substrate. The detailed dimensions are decided as: $a = 22.65$ mm, $b = 22.65$ mm, $L_c = 4.4$ mm, $L_u = 5.2$ mm, $L_s = 4.4$ mm, $I_1 = 5.3$ mm, $I_2 = 1.9$ mm, $W_o = 1.55$ mm, $W_u = 2.45$ mm, and $W_s = 0.45$ mm. The photograph of the fabricated filter is shown in Figure 6. By virtue of the single-cavity structure and flexible mixed coupling manner, the overall size of the fabricated filter is only 27.5 mm \times 27.5 mm \times 0.5 mm. An Agilent E8363B vector network analyzer is used for measurement. The measured and simulated frequency responses are illustrated in Figure 7. As can be seen, the measured results are in good agreement with the simulated ones. The measured central frequency is 10 GHz with a 3 dB fractional bandwidth of about 5.5%. The minimum passband insertion loss, including influence of the transition between the SMA connectors and microstrip as well as conductor and dielectric losses is about 1.98 dB, and in-band return loss is greater than 15 dB. Three transmission zeros are located at 8.2 GHz with 39.5 dB rejection, 9.15 GHz with 41 dB rejection, and 10.65 GHz with 40 dB rejection, respectively. By comparing three transmission zeros between measured and simulated results, only a small frequency shift on TZ3 and a spurious transmission zero are observed. The frequency shift is due to the fabrication tolerance between the actual and nominal value of the relative dielectric constant in high frequency. In addition, influence of the transition between the SMA connectors and microstrip may result in a spurious transmission zero. Overall, the proposed filter exhibits good frequency selectivity and compact size by profit from its single-cavity and MSLC structure.

4. CONCLUSION

An effective method to design single-cavity dual mode SIW filters with improved stopband characteristics is presented. By introducing mixed coupling between source and load of the proposed structure, three transmission zeros are generated in the stopband to improve the frequency selectivity. A filter sample has been designed and measured to validate the proposed method, and good agreement between the simulated and measured S -parameters is obtained. It is expected that the proposed filter will find applications in high-performance and high-integration microwave circuit design.

ACKNOWLEDGMENT

This work was supported by the National Natural Science Foundation of China (Grant Nos. 51172034, 61201001), and Fundamental Research Funds for the Central Universities of China (Grant No. ZYGX2011J132).

REFERENCES

1. Gao, M.-J., L.-S. Wu, and J.-F. Mao, "Compact notched ultra-wideband bandpass filter with improved out-of-band performance using wuasi electromagnetic bandgap structure," *Progress In Electromagnetics Research*, Vol. 125, 137–150, 2012.
2. Cui, D., Y. Liu, Y. Wu, S. Li, and C. Yu, "A compact bandstop filter based on two meandered parallel-coupled lines," *Progress In Electromagnetics Research*, Vol. 121, 271–279, 2011.
3. Chen, C.-H., C.-S. Shih, T.-S. Horng, and S.-M. Wu, "Very miniature dual-band and dual-mode bandpass filter designs on an integrated passive device chip," *Progress In Electromagnetics Research*, Vol. 119, 461–476, 2011.
4. Xu, Z., J. Guo, C. Qian, and W.-B. Dou, "A novel quasi-elliptic waveguide transmit reject filter for Ku-band VSAT transceivers," *Progress In Electromagnetics Research*, Vol. 117, 393–407, 2011.
5. Park, W.-Y. and S. Lim, "Bandwidth tunable and compact band-pass filter (BPF) using complementary split ring resonators (CSRRS) on substrate integrated waveguide (SIW)," *Journal of Electromagnetic Waves and Applications*, Vol. 24, Nos. 17–18, 2407–2417, 2010.
6. Chen, X. P., K. Wu, and D. Drolet, "Substrate integrated waveguide filter with improved stopband performance for satellite

- ground terminal,” *IEEE Trans. Microw. Theory Tech.*, Vol. 57, No. 3, 674–683, 2009.
7. Jiang, W., W. Shen, L. Zhou, and W.-Y. Yin, “Miniaturized and high-selectivity substrate integrated waveguide (SIW) bandpass filter loaded by complementary split-ring resonators (CSRRLs),” *Journal of Electromagnetic Waves and Applications*, Vol. 26, Nos. 11–12, 1448–1459, 2012.
 8. Wei, C.-L., B.-F. Jia, Z.-J. Zhu, and M.-C. Tang, “Design of different selectivity dual-Mode filters with E-shaped resonator,” *Progress In Electromagnetics Research*, Vol. 116, 517–532, 2011.
 9. Xia, B. and J. Mao, “A dual mode filter with wideband suppression,” *Journal of Electromagnetic Waves and Applications*, Vol. 26, Nos. 11–12, 1470–1475, 2012.
 10. Jedrzejewski, A., N. Leszczynska, L. Szydowski, and M. Mrozowski, “Zero-pole approach to computer aided design of in-line SIW filters with transmission zeros,” *Progress In Electromagnetics Research*, Vol. 131, 517–533, 2012.
 11. Chen, X. P. and K. Wu, “Substrate integrated waveguide cross-coupled filter with negative coupling structure,” *IEEE Trans. Microw. Theory Tech.*, Vol. 56, No. 1, 142–149, 2008.
 12. Zhang, Q.-L., W.-Y. Yin, S. He, and L.-S. Wu, “Evanescent-mode substrate integrated waveguide (SIW) filters implemented with complementary split ring resonators,” *Progress In Electromagnetics Research*, Vol. 111, 419–432, 2011.
 13. Shen, W., W. Y. Yin, and X. W. Sun, “Miniaturized dual-Band substrate integrated waveguide filter with controllable bandwidths,” *IEEE Microw. Wireless Compon. Lett.*, Vol. 21, No. 8, 418–420, 2011.
 14. Wu, L. S., X. L. Zhou, W. Y. Yin, L. Zhou, and J. F. Mao, “A substrate-integrated evanescent-mode waveguide filter with nonresonating node in low-temperature co-fired ceramic,” *IEEE Trans. Microw. Theory Tech.*, Vol. 58, No. 10, 2654–2662, 2010.
 15. Xiang, Q.-Y., Q. Feng, and X.-G. Huang, “Half-mode substrate integrated waveguide (HMSIW) filters and its application to tunable filters,” *Journal of Electromagnetic Waves and Applications*, Vol. 25, Nos. 14–15, 2043–2053, 2011.
 16. Shen, W., W.-Y. Yin, X.-W. Sun, and J.-F. Mao, “Compact coplanar waveguide-incorporated substrate integrated waveguide (SIW) filter,” *Journal of Electromagnetic Waves and Applications*, Vol. 24, No. 7, 871–879, 2010.
 17. Wu, L.-S., J.-F. Mao, W. Shen, and W.-Y. Yin, “Extended

- doublet bandpass filters implemented with microstrip resonator and full-/half-mode substrate integrated cavities,” *Progress In Electromagnetics Research*, Vol. 101, 203–216, 2010.
18. Shen, W., L. S. Wu, X. W. Sun, W. Y. Yin, and J. F. Mao, “Novel substrate integrated waveguide filters with cross coupling (MCC),” *IEEE Microw. Wireless Compon. Lett.*, Vol. 19, No. 11, 701–703, 2009.
 19. Wang, R., L. S. Wu, and X. L. Zhou, “Compact folded substrate integrated waveguide cavities and bandpass filter,” *Progress In Electromagnetics Research*, Vol. 84, 135–147, 2008.
 20. Zhang, Z. G., Y. Fan, Y. J. Cheng, and Y.-H. Zhang, “A novel multilayer dual-mode substrate integrated waveguide complementary filter with circular and elliptic cavities (SICC and SIEC),” *Progress In Electromagnetics Research*, Vol. 127, 173–188, 2012.
 21. Li, R. Q., X. H. Tang, and F. Xiao, “Substrate integrated waveguide dual-mode filter using slot lines perturbation,” *Electron. Lett.*, Vol. 46, No. 12, 845–846, 2010.
 22. Li, R. Q., X. H. Tang, and F. Xiao, “An novel substrate integrated waveguide square cavity dual-mode filter,” *Journal of Electromagnetic Waves and Applications*, Vol. 23, Nos. 17–18, 2523–2529, 2009.
 23. Shen, W., X. W. Sun, W. Y. Yin, J. F. Mao, and Q. F. Wei, “A novel single-cavity dual mode substrate integrated waveguide filter with non-resonating node,” *IEEE Microw. Wireless Compon. Lett.*, Vol. 19, No. 6, 368–370, 2009.
 24. Qin, P.-Y., C.-H. Liang, B. Wu, and T. Su, “Novel dual-mode bandpass filter with transmission zeros using substrate integrated waveguide cavity,” *Journal of Electromagnetic Waves and Applications*, Vol. 22, Nos. 5–6, 723–730, 2008.
 25. Zhang, Z. G., Y. Fan, Y. J. Cheng, and Y.-H. Zhang, “A compact multilayer dual-mode substrate integrated circular cavity (Sicc) filter for X-band application,” *Progress In Electromagnetics Research*, Vol. 122, 453–465, 2012.
 26. Amari, S. and U. Rosenberg, “A universal building block for advanced modular design of microwave filters,” *IEEE Microw. Wireless Compon. Lett.*, Vol. 13, No. 12, 541–543, 2003.
 27. Chu, Q. X. and H. Wang, “A compact open-loop filter with mixed electric and magnetic coupling,” *IEEE Trans. Microw. Theory Tech.*, Vol. 56, No. 2, 431–439, 2008.